Master of Science

Effect of water-based binders on the performance of carbon electrochemical double-layer capacitor

The Graduate School of University of Ulsan

School of Chemical Engineering

Seul Lee

Effect of water-based binders on the performance of carbon electrochemical double-layer capacitor

Supervisor: Professor Eun-Suok Oh

A Dissertation

Submitted to
The Graduate School of the University of Ulsan
In partial Fulfillment of the Requirements
For the Degree of

Master

by

Lee, Seul

School of Chemical Engineering
University of Ulsan, Korea
February 2018

Effect of water-based binders on the performance of carbon electrochemical double-layer capacitor

This certifies that the master's thesis

of Seul Lee is approved.

Committee Chair Prof. Seung Hyun Hur

Committee Member Prof. Won Mook Choi

Committee Member Prof. Eun-Suok Oh

School of Chemical Engineering

University of Ulsan, Korea

February 2018

Abstract in Korean

본 연구에서는 다양한 상업용 수분산 바인더 SBR(styrene-butadiene rubber), PTFE(polytetrafluoroethylene), CMC(carboxy-methyl cellulose)를 전기 이중층 커패시터의 활성탄소 소재 전극에 적용하였으며, 최적 바인더의 비율 및 특성 분석에 관한 연구를 수행하였다.

전기 이중층 커패시터는 안정적인 에너지 밀도와 높은 출력 밀도로 고출력의 에너지 공급이 가능하며 이차전지와 비교하여 충전 및 방전시간과 전지 수명에 있어서도 보다 우수하다. 전극 활성 물질, 전해질, 분리막과 같은 주요 소재에 비하여 바인더 연구는 많이 진행되고 있지는 않으나 이에 대한 관심은 꾸준히 증가하고 있다. 산업 현장에서는 주로 PVdF(poly vinylidene fluoride)를 기존 바인더로 사용하고 있으나 환경 오염 문제로 수분산 바인더에 대한 수요가 오르고 있다. 이에 본 연구에서는 기존 커패시터보다 장기간 에너지 충*방전이 가능한 전기 이중층 커패시터용 수분산 바인더를 목표로 하며, 바인더의 최적 비율과 특성을 분석하기 위해 충방전 특성, 율속 성능, Cyclic Voltammetry (CV), Electrochemical Impedance Spectroscopy (EIS) 등 다양한 전기화학적 분석과 물리화학적 분석을 실시하였다.

Abstract in English

In comparison to lithium ion batteries, EDLCs are superior to rate of charging/discharging as well as extremely stable cyclic energy density. Their main components such as active materials and electrolytes have been greatly studied, whereas the binder materials appropriate to EDLCs have not been much examined, even though many industrial companies are interested in the characteristic of binders. Most of manufacturing industry has used PVDF (polyvinylidene fluoride) as the binder of EDLCs. Unfortunately, the binder causes envionmental issues due to the use of an organic solvent, n-Methylpyrrolidone so that the manufacturer have tried to change the organic based binder to water based one.

In this study, various commercial water based binders such as SBR (styrene-butadiene rubber), PTFE (polytetrafluoroethylene), and CMC (carboxy-methyl cellulose) were applied to electrochemical double-layer capacitor (EDLC) composed of activated carbon electrodes. Their versatile characteristics in EDLCs are thoroughly investigated with different ratios of them. A variety of characterization techniques are applied to achieve our goal; cycle performance, rate capability, Cyclic Voltammetry (CV) and Electrochemical Impedance Spectroscopy (EIS), and some physicochemical analysis.

Contents

Figure list

Table list

1. Introduction

1.1. Electrochemical double-layer capacitors

Electrochemical double-layer capacitors (EDLCs) are charge storage device by using pseudo-capacitance which is generated by reversible faradaic redox reaction at the interface with electrode and electrolyte and electrochemical double-layer capacitance which is occurred by charge separation with electrostatic force at the electric double layer between with electrode and electrolyte. EDLCs can retain outstanding capacitance [Farad: F] as well as maintain both conventional electrostatic and electrolytic capacitor's characteristic. In terms of lithium system secondary battery, it does not have enough ability to provide high power energy, furthermore, it causes significant degrade of battery life when it operates on severe environment. Compared to lithium-ion secondary battery (LIB), EDLCs can offer high power density and has substantial properties in fast charging / discharging time, long life and cycle performance [1,2].

1.2. The principle, structure, and components of electrochemical double-layer capacitors

EDLCs consist of cathode, anode, electrolyte, separator and current collector. Cathode and anode materials are usually same so it called as symmetric EDLCs. In some special case, for instance, it can be used asymmetric electrodes to enhance the mechanical property or dielectric characteristic of EDLCs. The electrode's active materials are various like activated carbon, nanocomposite carbon, and metal oxide system. The most used one is activated carbon because it has the tremendous specific surface area, chemical resistance, low thermal expansion, high electrical conductivity and low cost. In the electrodes, the ions adsorb and desorb with physical reaction during cycling. The

electrolyte provides charge carrier in the ionic liquid phase. The separator has the role of the division for both cathode and anode by using a cellulose system porous membrane. The last component is current collector which is the way for charge flow. The EDLCs have a dielectric material between two counter electrodes.

In charge process, one of the electrodes has positive voltage by external force and then it becomes positive charged electrode that cation would be gathered. Another get negative voltage by anion and these processes will keep until the equilibrium of charge accumulation between cathode and anode. In charge process, both cathode and anode make special area called as an electric double layer which is located between electrode and electrolyte. In discharge process, both electrodes are connected with resistance and then the electrodes release electric charges as much charged as the amount. The current could flow in EDLCs system due to emitting of charge. In terms of EDLCs, they use F [Farad] as a unit [3,4].

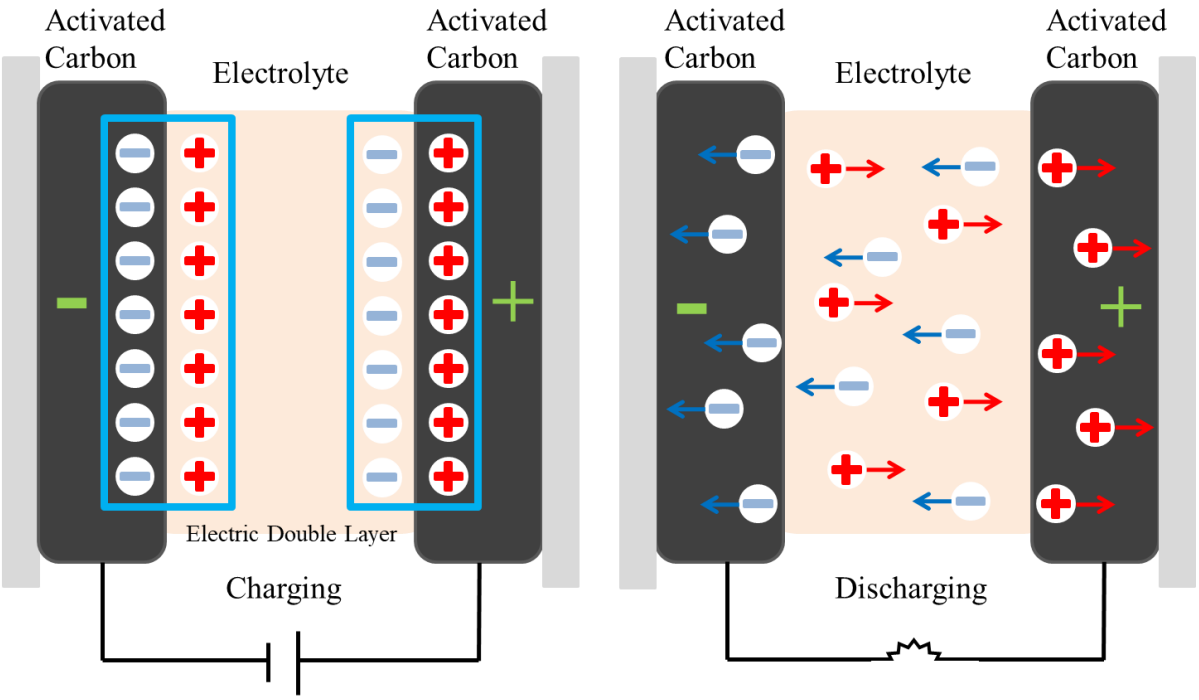

Figure 1. Schematic diagram of charging / discharging principle of electrochemical double-layer capacitors.

1.3. The characteristics of electrode materials

Activated carbon has been one of the most promising electrode materials for EDLCs because it has the high enormous specific surface area, stable chemical resistance, low thermal expansion, high electrical conductivity and cheap cost. Particularly, activated carbon has broad specific surface area and it would be a great advantage for EDLCs' capacitance during charging/discharging process. The activated carbon used experiment has 1500-1800 m^2/g total surface area, 0.7 ml/g pore volume, and 28 F/g theoretical specific capacitance. It is the powdered type for electric double-layer capacitors. It exhibits high adsorption capacity, controlled pore size distribution, high purity and low impurities. Compared to other active material such as silicon, lithium oxide, the activated carbon has low energy density. Despite low energy density, however, it has strong advantages for fast charge and discharge and superior power density, therefore, it has applied to various fields like transport, military, and large-scale energy storage system [5,6].

1.4. The binders for electric double-layer capacitors

Although binder is a minute part of EDLCs, the roles of the binder are so significant for long life cycle to stabilize electrode. It holds the connection with between micrometers active materials and electrical conduct additives and coat electrode slurry on current collector. The performance of a polymer binder in electrodes is expected to depend on several requirements: (1) adhesive force between the electrode and the current collector, (2) the boundary between the polymer binder and the active particles, (3) relationship of the binder with the electrolyte and at last (4) binder mechanical properties. The first element of adhesion is logical because high adhesion force is firmly required to confirm

long cycle life of EDLCs. Among binders corresponded to above prerequisite, they can be classified 2 kinds, solvent-based and water-based polymer. PVdF (poly vinylidene fluoride) which used most of the commercial battery is the representative of solvent-based binder because of its good stability. On the other hand, the representatives of the water-based binder are SBR (styrene-butadiene rubber), PTFE (polytetrafluoroethylene), and CMC (carboxy-methyl cellulose) which are used for EDLCs' electrodes. They can be dissolved in water, so the binder solvents are environment-friendly material and low price not to recovery solvent. The SBR binder effects on stable adhesive strength between electrode slurry and current collector. The SBR binder has used a commercial binder in the industry. The PTFE binder has excellent chemical resistance, electrolyte resistance and outstanding mechanical properties, however, cannot apply for the process of the slurry as the sole binder because it does not dissolve in the solvent. The CMC binder could increase binding strength of the particles and electrical property for the electrodes. Yet, the mechanical properties of CMC binder are lower than another commercial binder. To enhance the mechanical property of electrode by using the CMC binder, it needs to add the special ingredient which has both electrical stability and mechanical flexibility. Of course, electrodes using the CMC binder are much cheaper, environmentally friendly and even electrochemically stable than electrodes using conventional PVDF binder. In addition to the electrochemical performance can be enhanced by the modification of CMC, such as the quantity or type of metal salts, the degree of substitution (DS) of carboxymethyl groups, and the use of other types of celluloses [1,7].

To use the binder to make the slurry increases the density of electrode. Usually, the electrical conductivity is improved by the increment of conducting path as the dense electrode can compactly fill the space among particles. However, the internal resistance of the cell is proportional to the resistance of electrode thus the component of binder in

the slurry process can affect the electrical property of the cell.

2. Experimental

2.1. Preparation of the electrodes

2.1.1. Electrodes using SBR and PTFE as binder

The carbon electrode slurry was composed of 85 wt. % of activated carbon (Kuraray Chemical Co., Ltd., Japan) as an active material, 8 wt. % of conductive additive, 3 wt. % of a binder including both SBR and PTFE, 2 wt. % of CMC and used distilled water solvent to adjust the viscosity of the slurry. The slurry was mixed with a homogenizer (Nihonseiki Kaisha Ltd., Japan) for an hour. Mixed slurry is coated on aluminum etching foil as current collector and dried in a convection oven at 60 ℃ for 30 min, and then put in a vacuum oven for a day at 80 ℃.

2.1.2. Electrodes using CMC as sole binder

To make the electrode slurry, the electrodes composed of 87 wt. % of activated carbon as an active material, 7 wt. % of super-P as a conductive material and 6 wt. % of CMC binder and used distilled water solvent to adjust the viscosity of the slurry. The slurry was mixed by a homogenizer (Nihonseiki Kaisha Ltd., Japan) for an hour. Mixed slurry is coated on aluminum etching foil as current collector and dried in a convection oven at 60 ℃ for 30 min, and then put in a vacuum oven for a day at 80 ℃.

2.2. Fabrication of 2032 coin-full cells

The 2032 coin-full cells (CR 2032) were assembled in an argon-filled glove box using the symmetry carbon electrodes which one has the role of the working electrode and another has the role of the counter electrode. Between both electrodes, we used porous polypropylene film as separator and gasket to hold the separator and spacer and wave ring to fill empty space. And a commercial electrolyte used was 1M tetraethylammonium tetrafluoroborate (TEABF4) in acetonitrile (AcN).

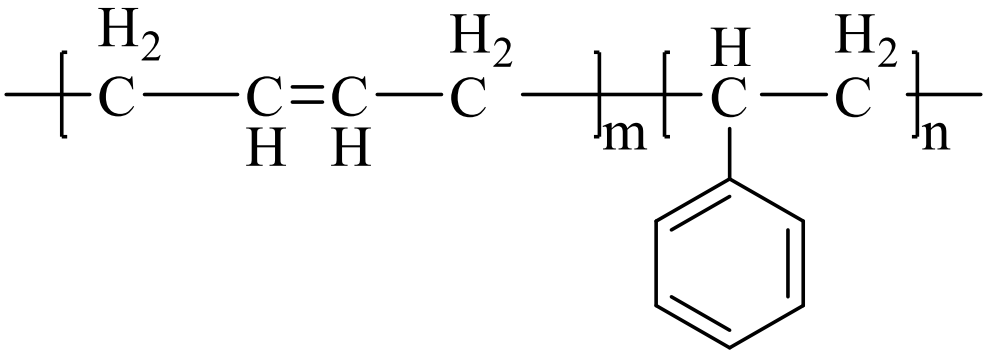

Figure 2. Chemical structure of styrene-butadiene rubber (SBR).

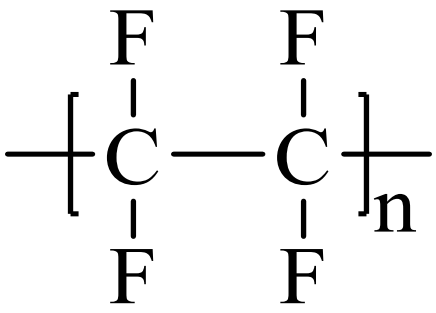

Figure 3. Chemical structure of polytetrafluoroethylene(PTFE).

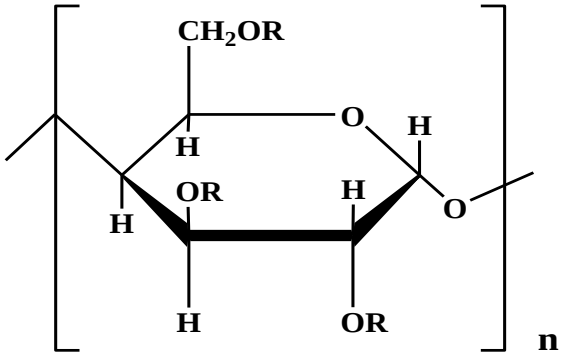

R=H or CH_2COOH

Figure 4. Chemical structure of carboxyl methyl cellulose (CMC).

Name of CMC	Average molecular weight	Degree of substitution	Weight percent (%)
CMC90-L	90,000	0.7	3
CMC250-L		0.7	2
CMC250-M	250,000	0.9	3
CMC250-H		1.2	3
CMC700-M	700,000	0.9	1

Table 1. The MWs and DSs of the CMCs.

	Concentration (%)	Total Content (%)
Activated Carbon	100	85
Super P	100	8
SBR	40	5
PTFE	60	
CMC	1	2

Table 2. The composition of the electrode using SBR and PTFE as binders.

	Concentration(%)	Total Content(%)
Activated carbon	100	87
Super P	100	7
CMC 3wt% solution	3	6

Table 3. The composition of the electrode using CMC as sole binder.

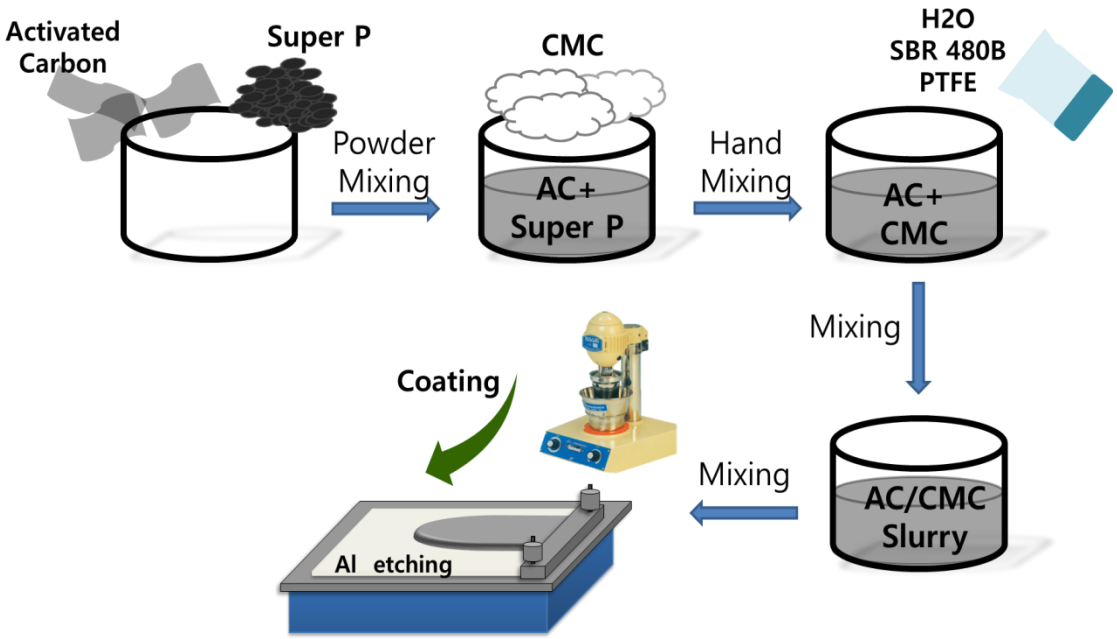

Figure 5. Schematic illustration of the manufacturing of electrode using SBR and PTFE as binders.

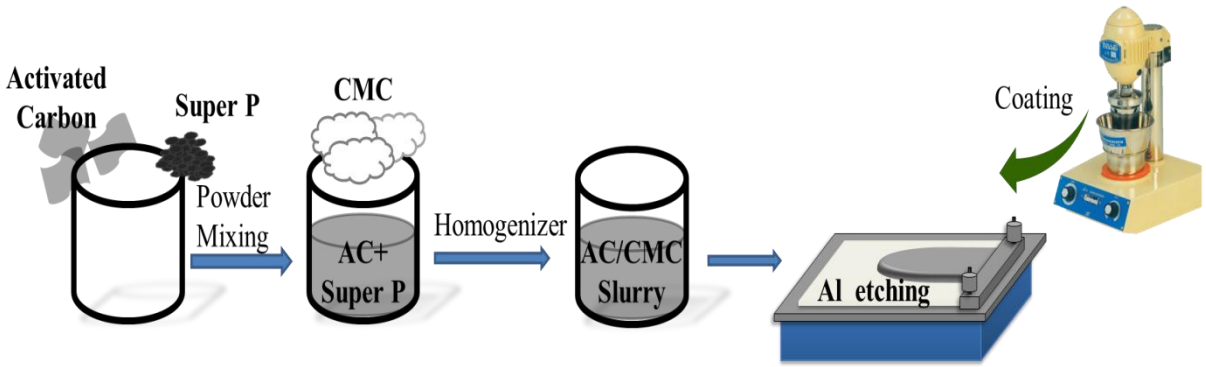

Figure 6. Schematic illustration of the manufacturing of electrode using CMC as sole binder.

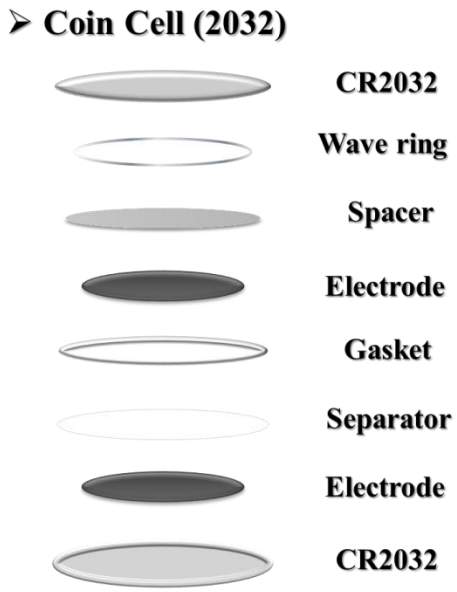

Figure 7. The components of 2032 coin-full cells.

2.3. Physicochemical characteristics

2.3.1. Adhesive strength

Mechanical adhesive strength between the electrode and current collector was estimated by 180° peel test using a texture analyzer (TA-PLUS, Lloyd Instrument Ltd.). For long life and stable capacity active material, adhesive strength is important. The adhesive strength was determined by measuring the electrodes before and after 24 hours soaking in the electrolyte's solvent. The electrodes after soaking were immersed in AcN. Sample preparation in the following ways: electrodes were cut rectangular form and their width was 2 cm. the electrodes were attached to double-side tape another side of the tape sticks on metal plate and they were pressed with the rolling machine for 2 times. Al etching foil was them peeled off using the top of the sample and the force was recorded during the experiment.

2.3.2. Thermogravimetric analysis (TGA)

Thermal stability was investigated by Thermogravimetric analysis (TGA) with a nitrogen atmosphere and 10 ℃/min heating, carried out by TA Instruments Q 50. The combinations of SBR and PTFE polymer film were dried and heated up to 800 ℃. A platinum pan was used to hold the sample

2.3.3. Brunauer-Emmett-Teller (BET)

Pore size distribution, pore volume, and surface area were measured by Brunauer Emmett-Teller (BET) with N_2 adsorption/desorption at -196 ℃, carried out by micromeritics ASAP 2020 adsorption analyzer and QUADRASORB evo. The pore size distributions of samples were analyzed by Horvath-Kawazoe (HK) and Barrett-Joyner-Halenda (BJH) method. A pretreatment temperature is 100 ℃ for SBR and PTFE and works for 30 hours. The pretreatment temperature is 200 ℃ for CMC and works for 50

hours, carried out by Xeri Prep degasser.

2.3.4. Contact angle

The polymer binder coated on Al etching foil and dried in a convection oven at 60 ℃ for 30 min. A specimen of 15π was cut and attached to a glass plate by a double-sided tape. The contact angle of thin binder film was measured by an optical tensiometer connecting with video device (Theta Lite 100, KSV Instrument Ltd., Finland) after the 40s exposing to a fixed amount of electrolyte droplet (1M $TEABF_4$ in AcN.) The device showed an angle between electrolyte droplet and the surface of binder film.

2.3.5. Field-emission scanning electron microscopy (FE-SEM)

The morphology of the surface of carbon electrode before and after cycling was observed by field-emission scanning electron microscopy (FE-SEM, JEOL JSM 6500F) with an Energy Dispersive X-ray spectroscopy (EDX). After cycling test, some cracks on electrode surface could be seen and the degree of cracks is different with depending on the ratio of binder or the component of the binder.

2.3.6. Ionic conductivity

The ionic conductivities of binder solutions containing an electrolyte's salt were also measured using a conductivity meter (S230-K, Mettler-Toledo).

2.4. Electrochemical characteristics

2.4.1. Galvanostatic charge and discharge test

The electrochemical properties were conducted by the cycling performances that were galvanostatically charged to 2.7V and discharged to 0.1V with constant voltage mode for 30 min from first to 5^{th} cycles. Consequently, after then the electrochemical performance of coin cells was measured by charge and discharge between 2.7V and 1.35V for observing long cycle life with a current mode at 10mA/F current. The rate capability test using a battery cycle device (PNE solution Co., Korea) was operated with each current 1, 5, 10, 50mA/cm^2 at the room temperature. In case of high temperature cycling test was conducted at 45 ℃ with the voltage range from 0.1V to 2.7V in a battery cycle device (WBCS3000, Wonatech, Korea).

2.4.2. Cyclic voltammetry (CV) and electrochemical impedance spectroscopy (EIS)

Cyclic voltammetry (CV, VSP, BioLogic Science Instruments) of the electrode was measured at the various scan rates, 5,20, 50, 100 mV/s and electrochemical impedance spectroscopy (EIS, VSP, BioLogic Science Instruments) was measured at a frequency range 10^{-3} to 10^{6} Hz after numerous cycles.

3. Results and discussion

3.1. Physical characteristics

3.1.1. SBR and PTFE binders

To evaluate that the adhesion strength between fine active material including binders and current collector, we tested 180° peel test, as shown in Figure 8. Figure 8 indicates adhesion strength of carbon electrode using SBR and PTFE binder depending on each binder ratio, before and after soaking in the electrolyte for a day. The adhesion force of the binder is also an important factor for keeping contact between the electrode and current collector and between active materials and conducting materials, particularly for the long cycle life. In Figure 8, the electrode which has a large amount of SBR shows high adhesive strength, on the other hand, PTFE binder shows low adhesion strength, so SBR: PTFE = 1:3 sample has the lowest of the adhesive electrode.

The electrodes soaked into the electrolyte were conducted without any salt, $TEABF_4$, at the room temperature for a day. After soaking, all of the electrodes indicate less adhesive strength than fresh electrodes. In particular, SBR: PTFE = 2:2 and SBR: PTFE = 1:3 samples cannot record their adhesion after electrolyte uptakes because of little adhesion strength, in contrast to SBR: PTFE = 4:0 and SBR: PTFE = 3:1 samples still have adhesion. Especially the degree of decrement for SBR: PTFE = 4:0 much less than other ratio of binder samples due to the high quantity of SBR.

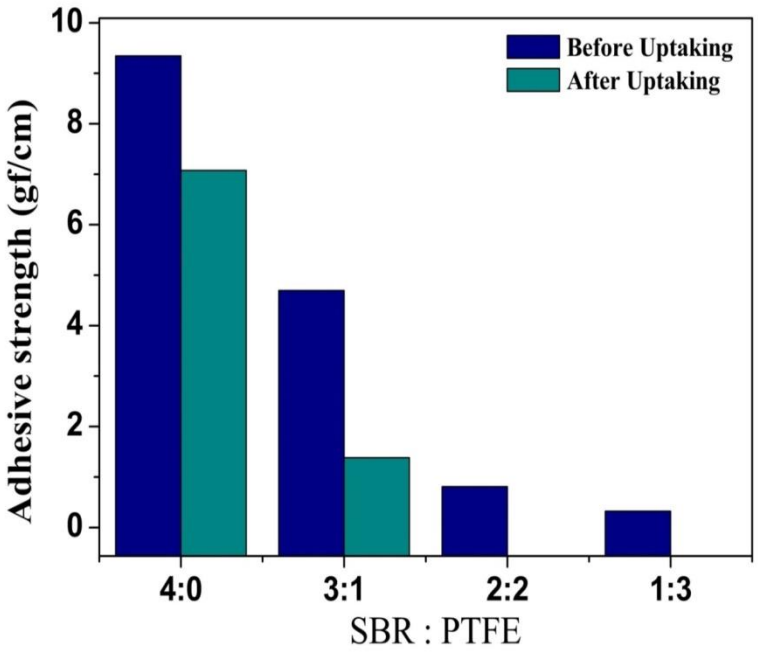

Figure 8. Adhesion strength of carbon electrode using SBR and PTFE binder depending on each binder ratio, before and after soaking in the electrolyte for 1 day.

To measure a thermal stability of SBR and PTFE, TGA was carried out at the temperature range from 25℃ to 800℃ with that the ramping rate is 10℃/min. The results of TGA are displayed in Figure 9, pure SBR and PTFE have almost one peak but the combinations of SBR and PTFE binder have two peaks. From these results, thermal degradation of SBR occurs around 390℃ and that of PTFE occurs around 580℃. At these temperatures, pure SBR and PTFE loss more than 99% weights of their initial weights. Indeed, PTFE has more thermal stability than SBR at the high temperature, so usually PTFE has been widely used for heating applications. Figure 9 shows that each ratio of binder has expected a result. From the weight loss amount, the first and second weight loss of SBR: PTFE = 3:1 is same as the ratio of the binder. Also SBR:PTFE = 2:2, 1:3 have same results. These results are reflected in the thermal stability of SBR and PTFE polymer property.

As consider the results of TGA, the electrode which contains more PTFE amount of binder would show much better cyclic performance at the high-temperature environment because of the fluorinated thermoplastics binder, PTFE, has good thermal stability than SBR [1,6].

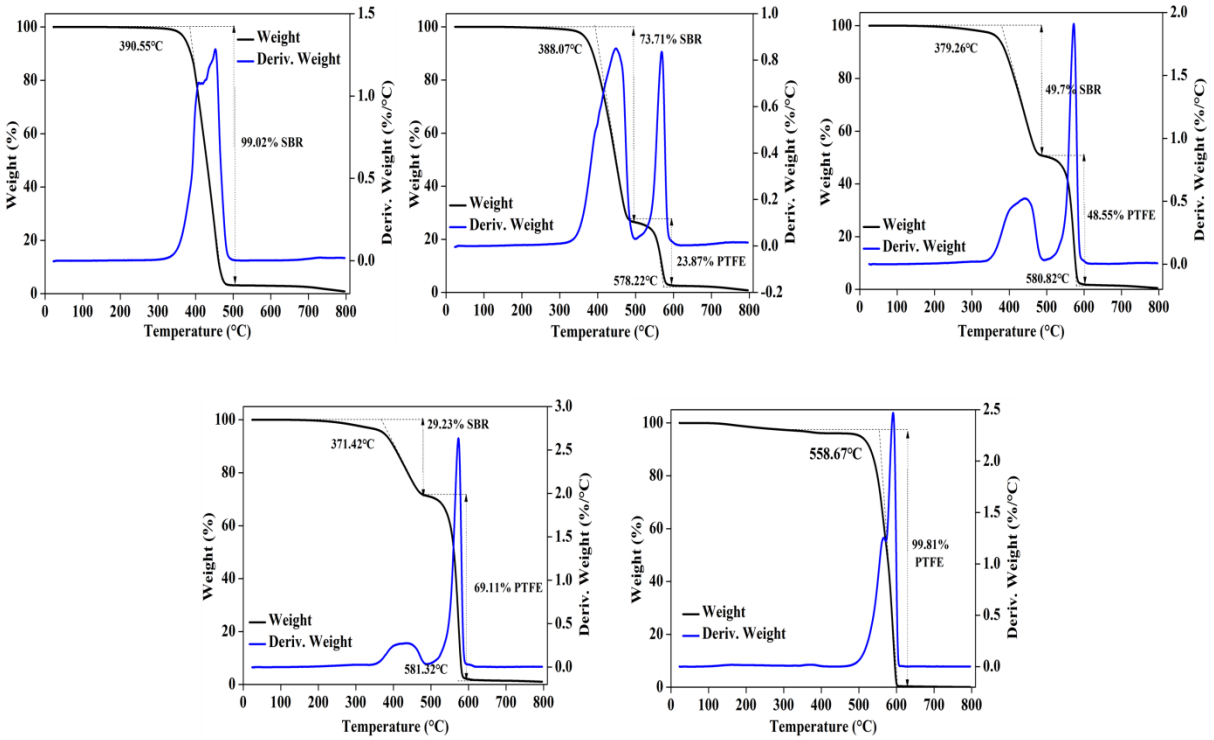

Figure 9. Loss of weight (%) for the binder ratio of SBR and PTFE. TGA temperature range from room temp(25℃) to 800℃.

One of the crucial factors for supercapacitor's behavior is specific surface area of active materials. While supercapacitor charge and discharge by exterior electric force, electrolyte ions enter into the activated pores. Therefore, the specific capacitance for supercapacitor is related to the specific surface area of activated carbon material or the pore size distribution and the moving ion size of the electrolyte. The activated carbon used as active material in symmetric carbon electrodes has tremendous specific area because of an uncountable number of micro-pores. According to the results in Table 4, BET surface area of electrode decrease as electrodes contain more amount of PTFE. Also, total pore volume which directly affects the specific capacitance decreases. The noticeable trend in BET results is the variation of the specific surface area of mesopores. In case of mesopores, it is the route for electrolyte ions to charge electrochemical energy. The specific capacitance of supercapacitor would increase when the surface area of mesopores is activated well. It was demonstrated that the SBR: PTFE = 4:0 has higher specific capacitance than other samples in Table 4, and it has broad specific surface area of mesopores contrast with other samples. In a recent paper, it is manifested that it is arduous for electrolyte ions to go through the micro-pores because their diameter (< 2nm) is too narrow. However, mesopore has a large diameter (2-50nm), so it is more convenient for ions to move from buffer solution to electrochemical double layer. Pore diameter distribution is shown in Figure 10. Pure activated carbon has wide pore diameter distribution but SBR: PTFE = 1:3 has narrow dispersion. It means that PTFE particle would block micro-pores as well as mesopores [8,9].

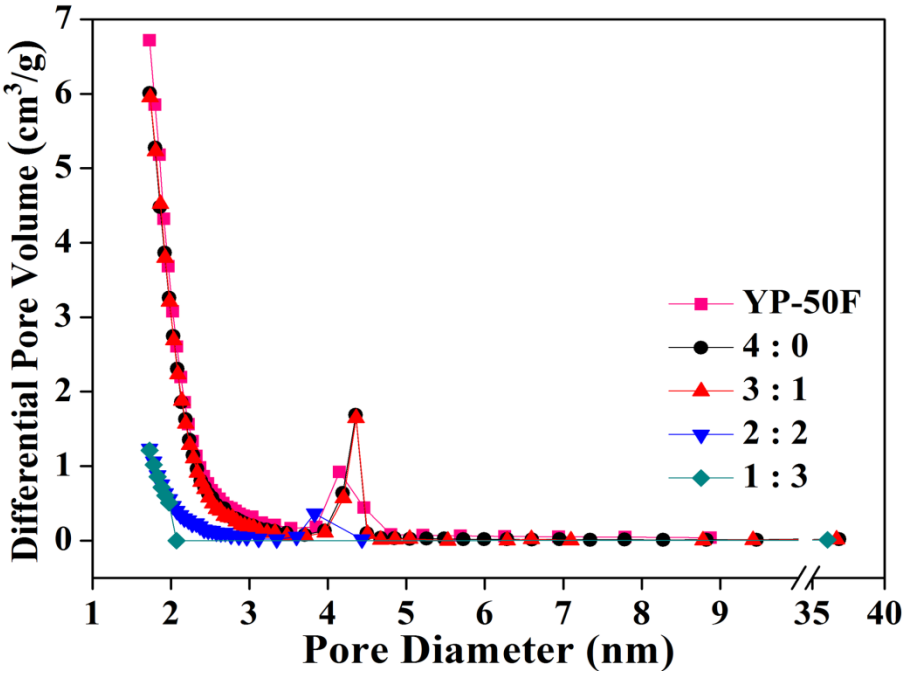

Figure 10. Pore diameter distribution curves based on the BJH method.

	HTT [°C]	S_{BET} [m^2g^{-1}]	S_{micro} [m^2g^{-1}]	S_{meso} [m^2g^{-1}]	V_{total} [cm^3g^{-1}]
YP - 50F	350	1701	1463	238	0.752
SBR : PTFE = 4 : 0	100	1432	1181	251	0.625
SBR : PTFE = 3 : 1	100	1427	1269	158	0.613
SBR : PTFE = 2 : 2	100	1387	1282	105	0.587
SBR : PTFE = 1 : 3	100	1344	1259	84	0.545

Table 4. BET surface area and total pore volume for active material containing SBR and PTFE

The intrinsic characteristic of binder can be measured by contact angle test between binder film and the electrolyte using 180° peel test device [7]. In the contact angle test, it is easy to know a wettability indicated interaction between binder and electrolyte, also it depends on the functional groups presenting on its surface. As seen in Figure 11 (a), at first of experiment, PTFE shows high contact angle with electrolyte around θ = 55°, SBR and PTFE become similar to each other in the course of time. Both of SBR and PTFE have final contact angle, around θ = 25°, and it means that SBR and PTFE have fine interaction with electrolyte, however, good wettability could cause diminishment of binder adhesion. In Figure 11(b), it takes around 40s to be stabilization and it is necessary to estimate contact angle. Basically, the contact angle is the angle between gas or liquid drop and solid surface when droplet has a thermodynamic equilibrium with a solid surface. High contact angle means low wettability and hydrophobic property, on the other hand, low contact angle corresponds to high wettability and hydrophilic property.

To study the configuration of supercapacitor electrodes, FE-SEM was carried out in Figure 12. Figure 12 (a) shows that the morphology of electrodes which is not treated with any experiment. These images display that the porous characteristics of the electrodes depending on the binder ratio between SBR and PTFE. It can be observed from the micrographs that the exterior surface of the activated carbons covers with conductive additives. Furthermore, the shape of the material is distinct and it is easy to know the dispersion of activated carbon and conductive powder is succeeded. The investigation of electrodes used for numerous cycling is shown in Figure 12 (b). To see the change of electrode morphology after 30000 cycles, the coin-full cells are disassembled and the electrodes are taken out from the coin cell. Compared to the fresh electrodes, the used electrodes have cracks, fissure and the obscure boundary among

materials. As the adhesive force mentioned in Figure 8, SBR has better adhesive property than PTFE. The SBR: PTFE = 4:0 sample has the highest adhesive strength than others, so the binder can hold all material each other. In addition to the interaction with active material and current collector is stable, consequently, that sample has no significant cracks compared to other samples. However, in case of SBR: PTFE = 1:3 sample, the electrode has significant crevices also the depth is deeper and deeper. During the reversible cycling, the electrolyte permeates into the materials, the physical structure of active material have destroyed and changed by a variety of mechanisms [10].

In this study, the main subject is analyzing the characteristic of binder in carbon-based supercapacitors. The charge storage process is happened by both electrostatic force and the electrolyte ions simultaneously absorbed/desorbed in the electrochemical double layer. It is critical part of binders that do not prevent the electrolyte ions from migrating through their own path during charging and discharging. $TEABF_4$ in acetonitrile used as the electrolyte has good ionic conductivity over than 35 mS/cm compared to other pure binders in Figure 13. The pure SBR and PTFE have tiny ionic conductivity because they do not contain any ions. To estimate how much pure binder increases their conducting ability for $TEABF_4$ ions compared to the commercial electrolyte, it processes that putting the $TEABF_4$ 1M into SBR and PTFE in order to make same concentration with commercial electrolyte. The binders adding salts exhibit that their ionic conductivities increase dramatically around 20mS/cm. Even though PTFE with salts more soar than SBR with salts, the terminal ionic conductivity of two binder solutions is similar each other. Compared to the electrolyte, two binder solutions are still lower than commercial one, but it could demonstrate that there is no much obstacle to ion's locomotion in binder solution during cycling [11].

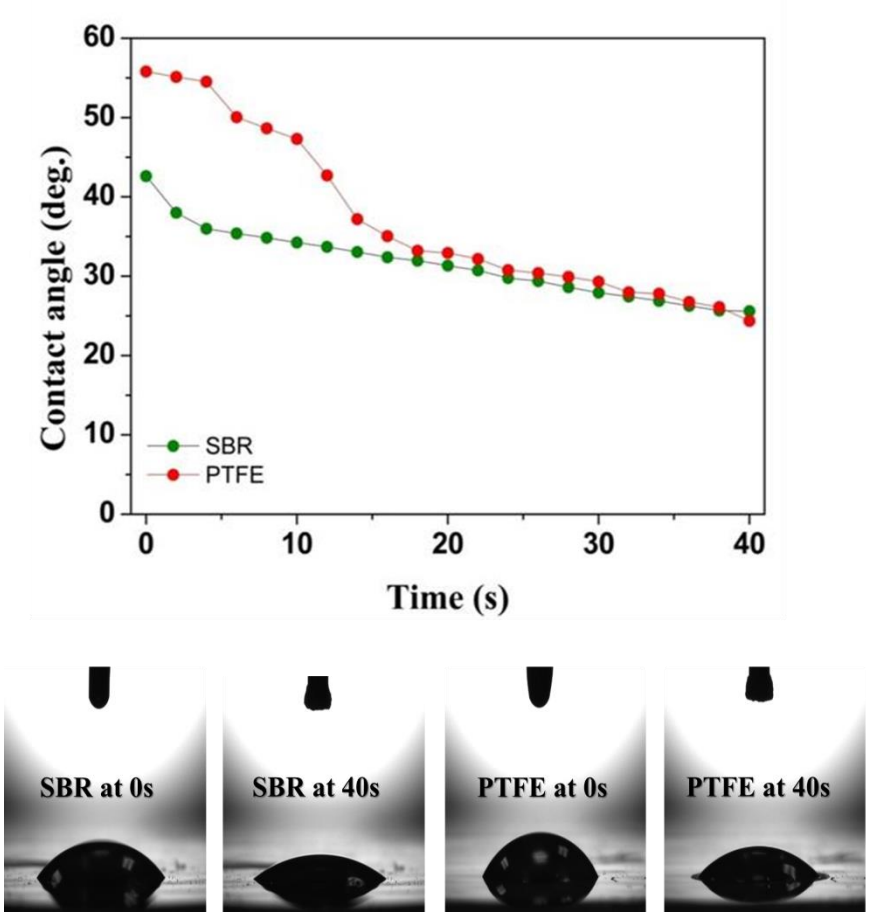

Figure 11. (a) Contact angles between binder films and electrolyte.

(b) Photographs of the moment that electrolyte was dropped at binder films after the 40s.

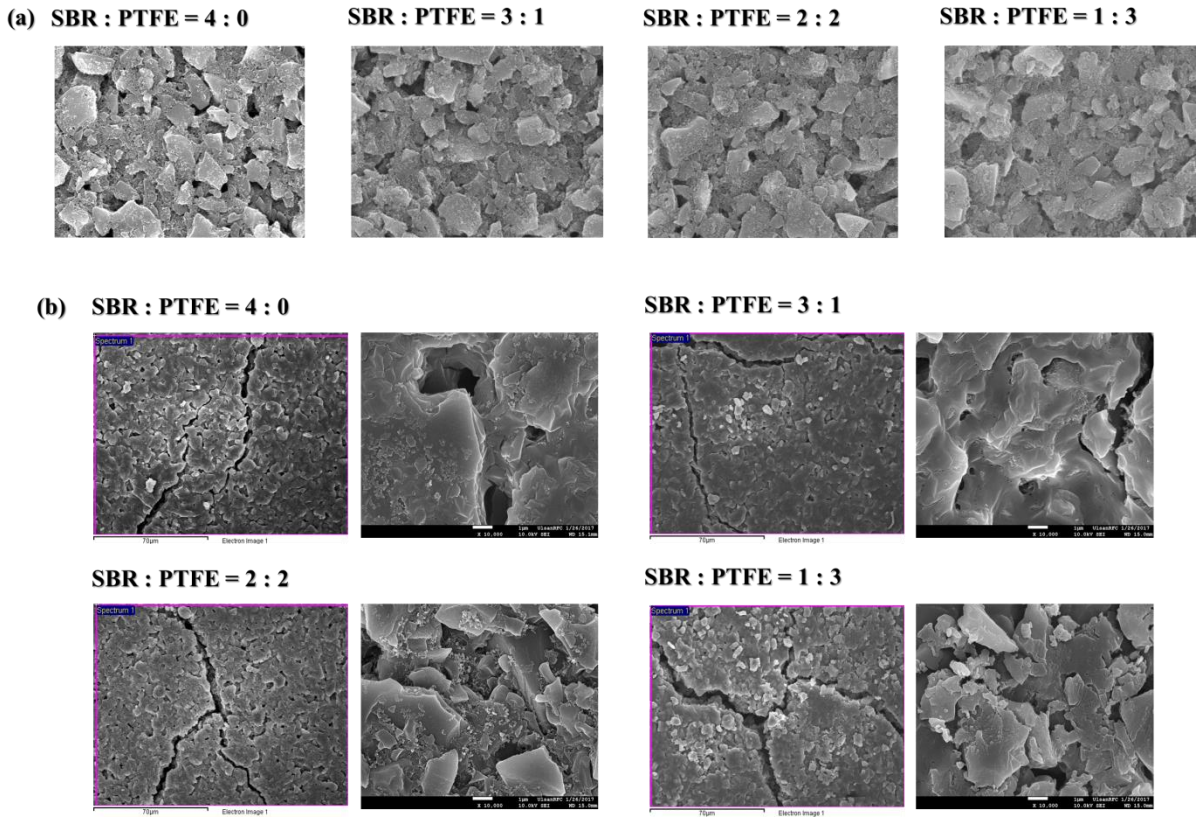

Figure 12. FE-SEM morphology of supercapacitor electrodes with different ratio of SBR and PTFE as used binder.

(a) original electrodes

(b) electrodes after 30,000 cycles.

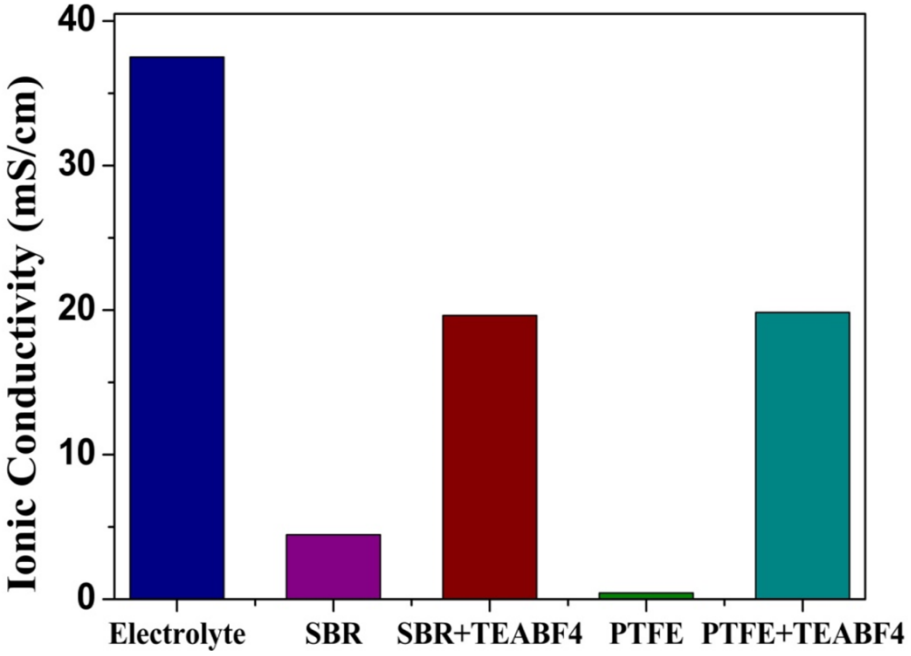

Figure 13. Ionic conductivity of the combination binder and salts ($TEABF_4$)

3.1.2. CMC binder

Figure 14 and 15 indicate adhesion strength of carbon electrode using CMC as sole binder depending on molecular weights and degree of substitution, before and after soaking in the electrolyte for a day. In case of the CMC-containing electrodes, the adhesion strength was in the order of CMC 700-M > CMC 250-H > CMC250M > CMC 250-L > CMC 90-L. As expected, an increment of MWs of CMC enhances the adhesive force both between fine activated carbon particles and between the active materials and Al etching foil. This might be attributed to the formation a more entanglement of structures in the electrode by longer polymer chains. Furthermore, it is clear from the results of CMC 250-containing electrodes that the degree of substitution affects the adhesion strength. The increment of DS improves the adhesive force of electrodes by the carboxyl functional group [-COOH]. High DS of CMC means a large number of carboxymethyl groups substituting for the hydroxyl groups [7,12].

The electrodes soaked into the electrolyte solution, acetonitrile, were conducted, at the room temperature for a day, shown in Figure 15. After soaking, all of the electrodes indicate little adhesive strength than fresh electrodes. All of CMC-containing electrodes cannot hold the materials each other and then they can easily be broken, so it is impossible to measure the adhesion strength of electrodes after electrolyte soaking. However, the strong adhesion strength might effect on the performance of EDLCs because the strong adhesive force can disturb by generating the internal resistance its cycle procedure of adsorption/desorption of electrons and ions by electrostatic force.

Surprisingly, the order of CMC binders regarding of the adhesion strength is totally not followed by the performance of cycle in contrast to SBR and PTFE electrodes. Moreover, the high adhesive force leads the electrodes to have lower capacitance than the electrodes having low adhesive force.

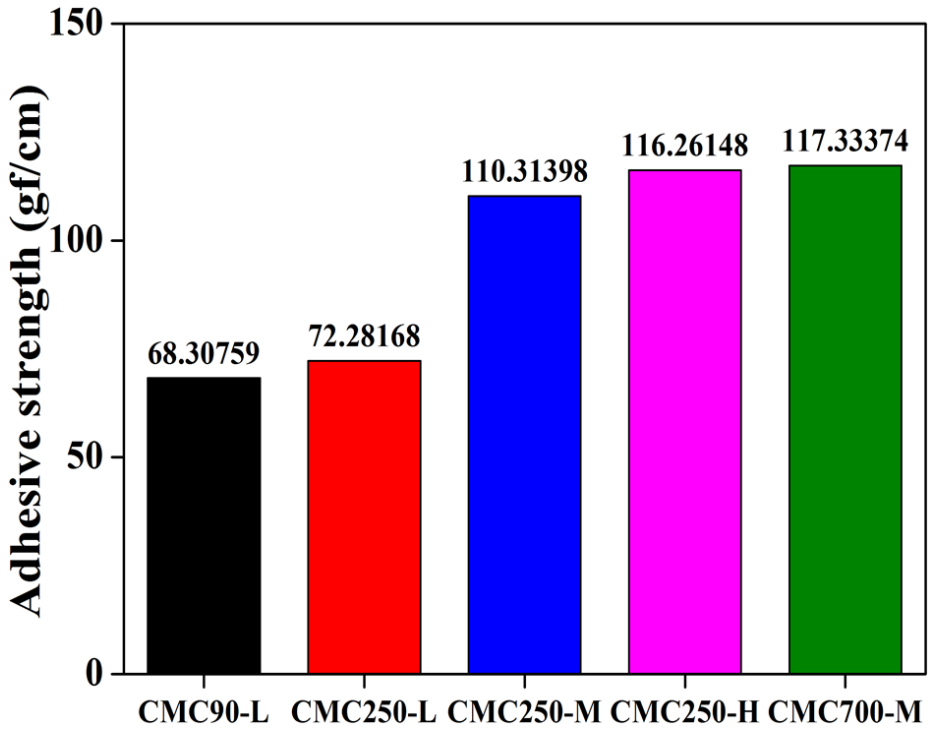

Figure 14. Adhesion strength of carbon electrode using CMC binder depending on MWs and DSs.

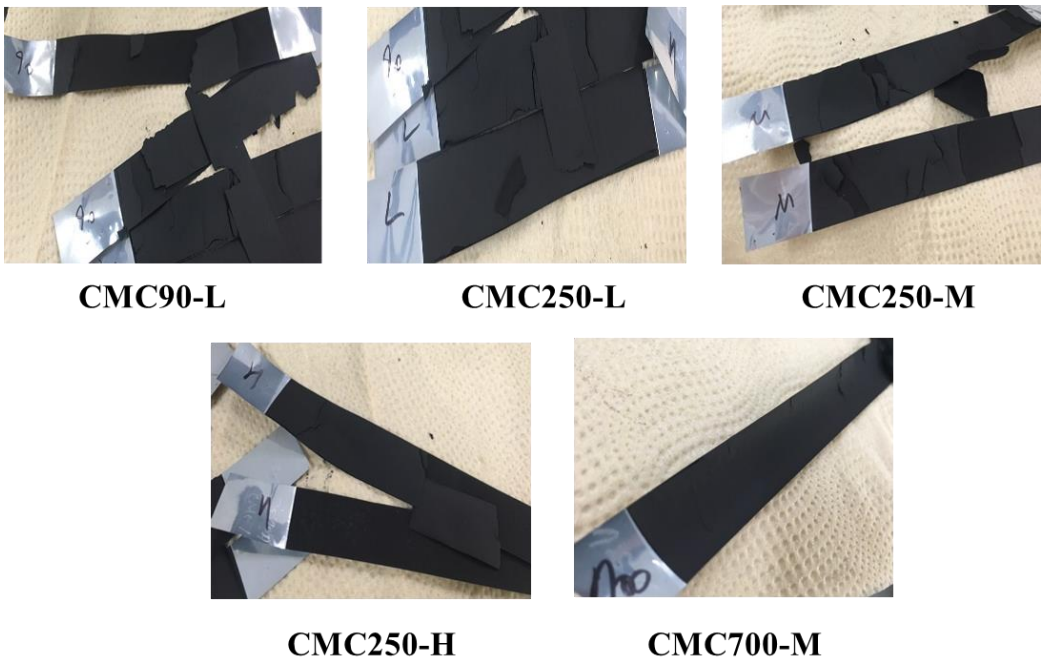

Figure 15. The photographs of electrodes using CMC binder after soaking into electrolyte for a day.

The specific capacitance for supercapacitor is related to the specific surface area of activated carbon or the pore size distribution and the moving ion size in the electrolyte. According to the results in Table 5, BET surface area of the electrode is not connected with any MWs and DSs of CMC binders but, the results in the order of surface area is exactly matched with the cycle capacitance. In terms of CMC-containing electrodes differ from SBR and PTFE-containing electrodes, the surface area of micro-pores directly influence the cycle performance. Hence, the CMC binders help the active material to utilize a large number of micro-pores then SBR and PTFE. Even though the size of mesopores is much proper to pass through the sophisticated way for ions, its impact is lower than micro-pores' one because the amounts of mesopores are still less than the huge amount of micro-pores. For the range of micro-pores, the HK method is used to calculate the distribution of pore diameter, and for the range of mesopores, the BJH method is used to calculate the distribution of pore diameter, shown in Figure 16 [10,13].

The affinity of between binder and electrolyte is the momentous factor for the electrochemical reaction. This intrinsic characteristic of binder means a wettability indicating an interaction between binder and electrolyte, also it can change depending on the functional groups presenting on its surface. As seen in Figure 17 (a), at the first moment of the experiment, high MW CMC and low DS CMC show high contact angle with electrolyte around $\theta = 20°$, low MW CMC and middle and high DS CMC have similar contact angle less than $\theta = 15°$. Compared to the contact angle of SBR and PTFE binder, CMC binders have a better relationship with electrolyte. Though CMC 700-M and CMC 250-L have higher contact angle than others, all of CMC binders indicate the contact angle less than $\theta = 20°$. Normally, the degree of contact angle does not care about magnitudes if the contact angle shows less than $\theta = 20°$, because it

means that better affinity between binder and electrolyte indicates around $\theta = 20°$ contact angle.

To study the configuration of supercapacitor electrodes, FE-SEM was carried out in Figure 18. Figure 18 shows that the morphology of electrodes that the porous characteristics of the electrodes depending on the MWs and DSs of CMC binder. It is not obvious from the micrographs to distinguish each electrode because the amounts of binder in total amount of electrode are very tiny and CMC binder is used by the solution type. From the micrographs, we can observe that the satisfying dispersion of active material and conductive material.

In the ionic conductivity, the salts, $TEABF_4$ put into the CMC binders and then make the 0.1M $TEABF_4$ in CMC binder solutions. In table 6, the electrolyte is commercial product having the concentration of 1M $TEABF_4$. This experiment just was carried out to see the tendency of ionic conductivity depending on the MWs and DSs of CMC. Ionic conductivity is in the order of CMC 250-H > CMC250M > CMC 700-M > CMC 90-L > CMC 250-L, shown in Figure 19. There are not many big gaps between CMC binders, but the high DS of CMC displays better ionic conductivity, and the high MW of CMC has lower ionic conductivity at the same molecular weights.

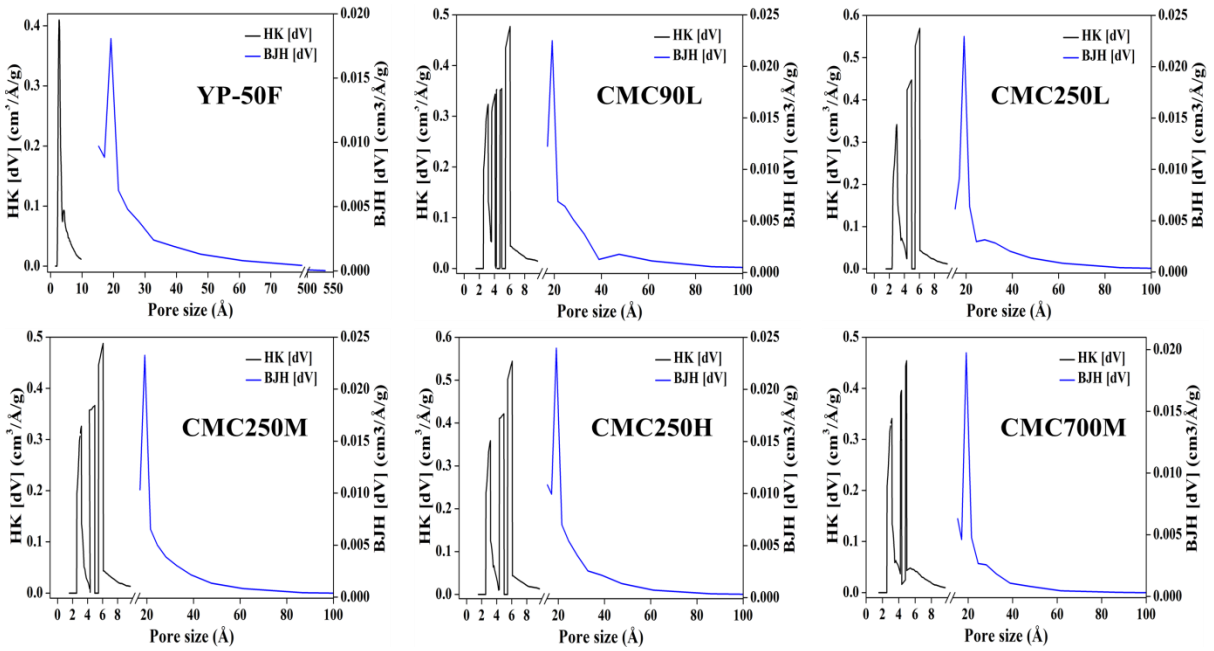

Figure 16. Pore diameter distribution curves based on the HK and BJH method.

	HTT [°C]	S_{BET} [m^2/g]	S_{meso} [m^2/g]	S_{micro} [m^2/g]	V_{micro} [cm^3/g]	V_{meso} [cm^3/g]	V_{total} [cm^3/g]
YP - 50F	300	1542	151.2	1390	0.613	0.191	0.804
CMC90-L	200	941	195	746	0.379	0.271	0.650
CMC250-L	200	1076	152.2	924	0.432	0.224	0.656
CMC250-M	200	967	152.3	815	0.383	0.253	0.636
CMC250-H	200	1043	177	866	0.418	0.236	0.654
CMC700-M	200	1019	117.2	901	0.399	0.177	0.576

Table 5. BET surface area and total pore volume for active material containing CMC

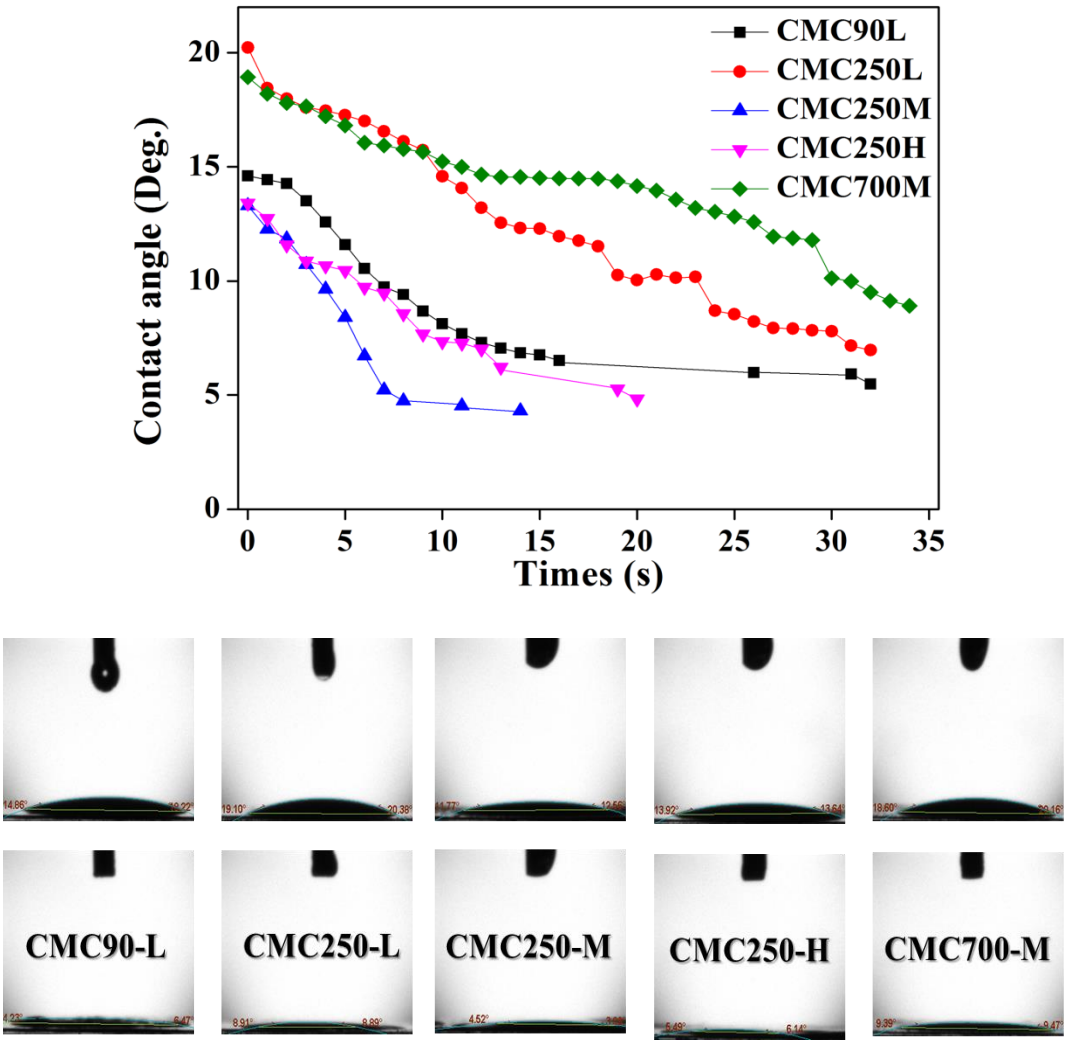

Figure 17. (a) Contact angles between binder films and electrolyte.

(b) Photographs of the moment that electrolyte was dropped at binder films after the 35s.

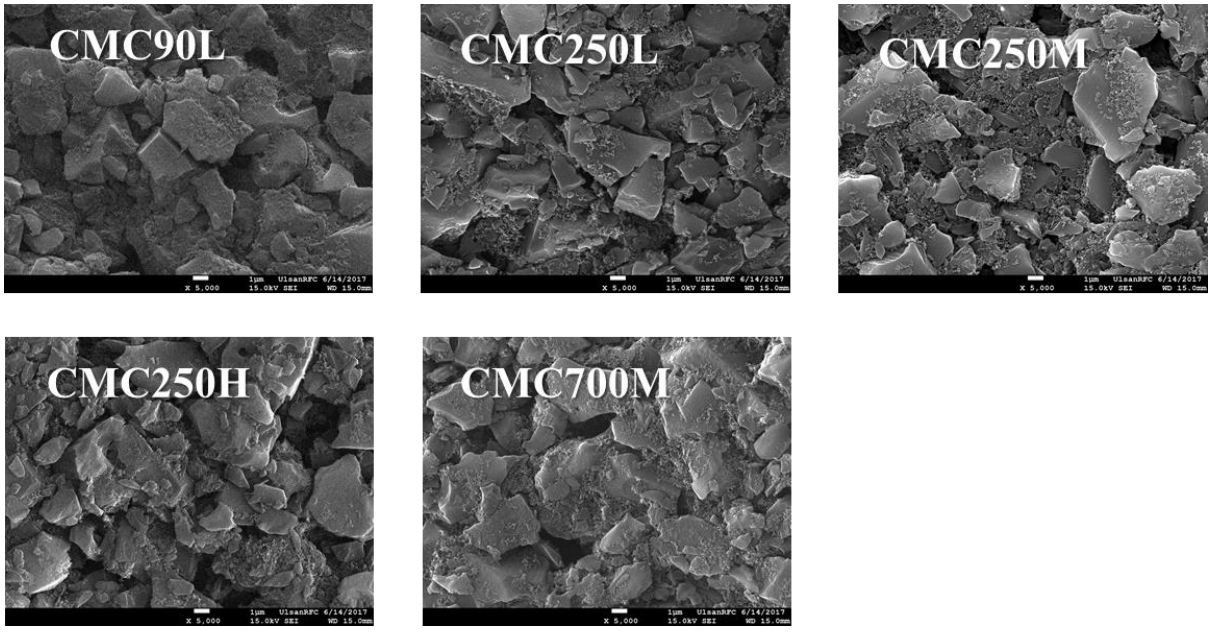

Figure 18. FE-SEM morphology of supercapacitor electrodes with different MWs and DSs of CMC

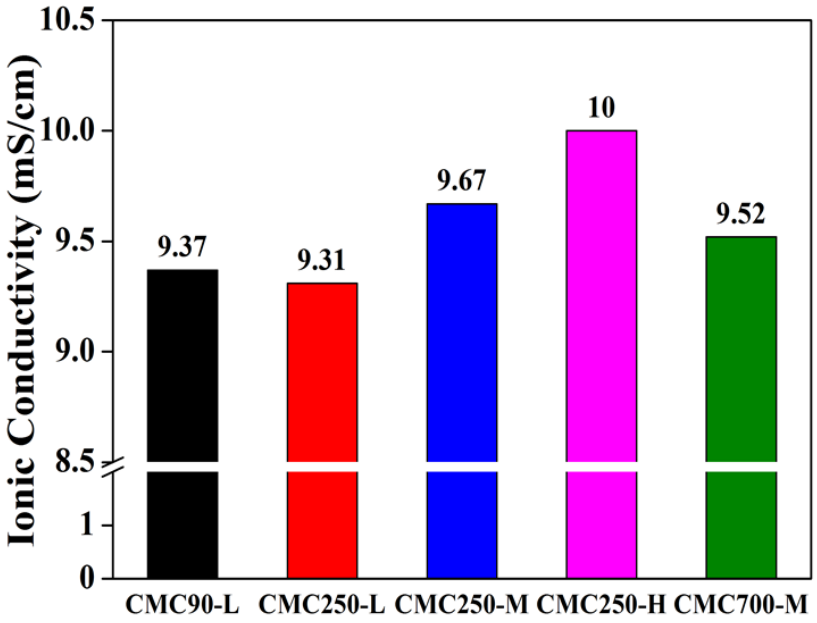

Ionic Conductivity (mS/cm)	Electrolyte	CMC90L	CMC250L	CMC250M	CMC250H	CMC700M
	56.2	9.37	9.31	9.67	10	9.52

Figure 19. The tendency of ionic conductivity of CMC binder solutions with salts ($TEABF_4$)

Table 6. Ionic conductivity of electrolyte (1M $TEABF_4$ in AcN) and binder solutions with 0.1M $TEABF_4$.

3.2. Electrochemical characteristics

3.2.1. The electrodes using SBR and PTFE binders

In this experiment, specific capacitance (F/g) of the electrodes containing each different binder ratio of SBR and PTFE is shown in Figure 20 [14]. When the electrode has large SBR amounts, the EDLCs electrode has the highest capacitance and shows stable performance in the cyclic test. During 30000 cycles, the specific capacitance of EDLCs gradually decreases, but a degree of capacitance reduction is not too much than expected. As to SBR: PTFE = 3:1 and SBR: PTFE = 2:2, 2:2 sample has larger capacitance than 3:1 at the beginning of cycling, but 3:1 sample has larger capacitance than 2: 2 at the end of cycles. It means that the adhesion force of supercapacitor binder is one of the important factors for long cycle life. When the cycle comes to 30,000 cycles, the adhesion force between the binder and current collect becomes more important. So, it can affect the cyclic performance of supercapacitor. In case of the SBR : PTFE = 1:3 electrode, it shows the lowest specific capacitance during all cycles and it is exactly match with the BET surface area in Table 4.

In the rate capability test of supercapacitor was conducted on the range of 0.1V to 2.7V and constant voltage time for 30miniutes per each cycle and the current changes for every 20 cycles with the current density, 1 mA/cm^2, 5 mA/cm^2, 10 mA/cm^2, 50 mA/cm^2 and then return to 1 mA/cm^2. As seen Figure 21, in the approximate order of the specific capacitance of rate capability test is similar to the results of the cyclic performance shown in Figure 20. In the high current density, all binder ratio electrodes decrease their specific capacitance. The SBR: PTFE = 3:1 sample shows the big change of specific capacitance reduction but it can recover to original specific capacitance over than 96%. All range of the current density, The SBR: PTFE = 4:0 sample indicates higher capacitance than others and it is the same result with the cyclic test. At the

beginning of 1mA/cm^2 current density, SBR:PTFE = 3:1 sample has bigger specific capacitance than SBR:PTFE = 4:0 sample. At final 1mA/cm^2 current density, however, SBR: PTFE = 4:0 sample has bigger specific capacitance than 3:1 sample. It means that 4:0 sample can stably maintain capacitance than 3:1 sample due to its strong adhesive strength. Take the other current densities, 4:0 sample shows the biggest specific capacitance but 1:3 sample has the lowest specific capacitance. For these conditions, supercapacitor needs powerful adhesive strength to operate itself in a wide range of fields where using low velocity of charging and discharging, also fast one.

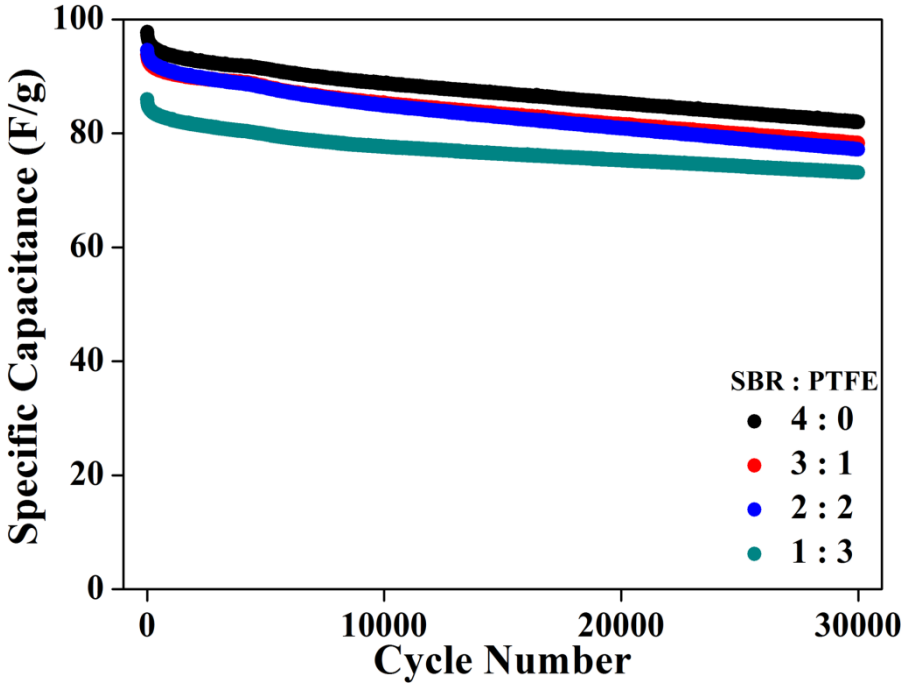

Figure 20. Cycling performance of the EDLCs using different ratio of binder between SBR and PTFE for 30,000 cycles

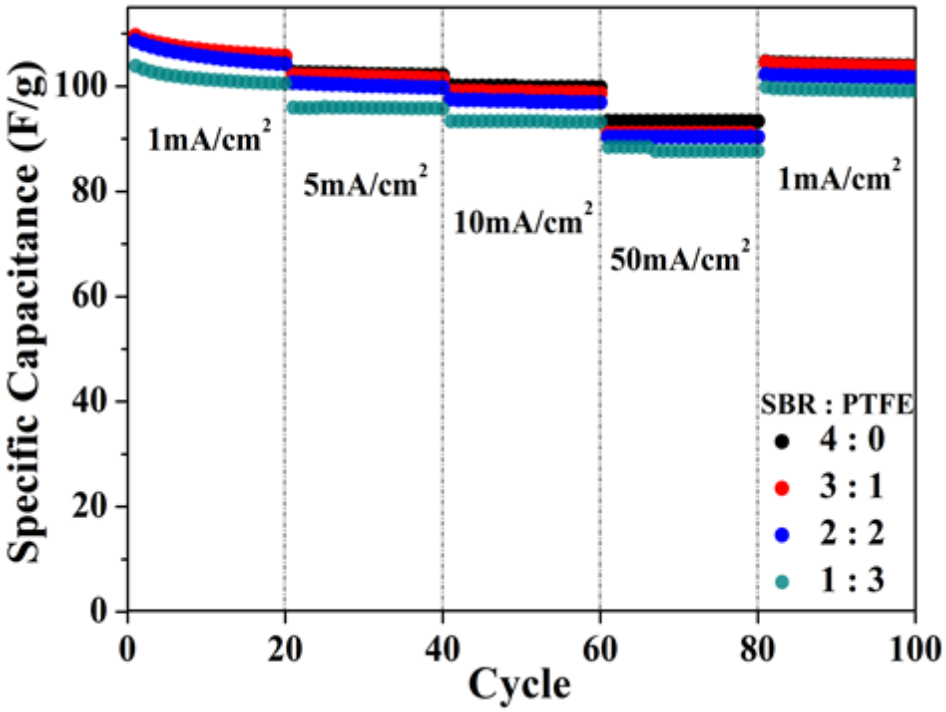

Figure 21. Performance of supercapacitor rate capability test. Current changes for 20cycles and voltage range from 0.1V to 2.7 V.

To know precisely how to get these cycle performance results, it is essential that measure the electrochemical impedance spectroscopy (EIS) test. In EIS results, we can compare the resistance of each binder ratio. Figure 22 and the inset illustrate an impedance spectrum of the EDLCs after 10,000 charge/discharge to investigate the effect of SBR and PTFE binder on the resistances of the supercapacitor electrodes. The frequency ranges from 10^{-2} to 10^{6} Hz at 0V. There are three distinctive regions depending on the frequency in Nyquist plot of EIS test. At low frequency, it demonstrates the behavior of pure capacitors and is related to the imaginary part. Generally, the line sharply increases and shape likes vertical controlled by mass transfer. At high frequency, the performance of supercapacitor looks like a pure resistance. In the middle frequency region, a semicircle expresses the magnitude of diffusion resistance by diffusion procedure of that the ions penetrate into the porosity of electrode active materials. And the domain is controlled by a kinetic mechanism [15,16]. The SBR: PTFE = 1:3 sample has relatively large charge transfer resistance according to the size of semicircle in the middle-frequency region. SBR: PTFE = 1:3 sample is in contrast with other three binders ratio but all Nyquist plots have a similar shape. In the low-frequency region, on the other hand, all samples draw virtually vertical line that means these EDLCs have high capacitance and normal capacitor character [13]. In terms of the equivalent series resistance (ESR), the first intercept at the real part axis of the Nyquist plot, represents the entire resistance from the electrolyte solution, the active material of the electrode, and the contact resistance of the interface between the electrode and the current collector [17,18]. The ESRs of supercapacitor is very low. The SBR:PTFE = 4:0 sample has 0.52Ω, 3:1 sample has 0.522 Ω, 2:2 has 0.43Ω, and 1:3 sample has 0.588 Ω. Given the results of semicircle diameter and ESR, SBR: PTFE = 1:3 samples have the large impedance that needs big

energy to move both ions and electrons between electrolyte solution and electrode. Compared to SBR: PTFE = 1:3 sample, the other samples have a small impedance in order of binder ratios.

Compared to the effects of resistance's combination, SBR: PTFE = 4:0 sample has the smallest resistance, and it matches with the result of Nyquist plots. In terms of Nyquist plots, as a large amount of SBR binder increases, the resistance decreases conspicuously. Those facts can comply with the axiomatic tendency of active surface areas in carbon material. In this regard, supercapacitor should consider how amount of binder particles suffuse active materials

Cyclic voltammetry (CV) was carried out to scrutinize the performance of supercapacitor over a voltage window between 0 and 3 V, with different scan rates. Figure 23 presents the cyclic voltammetry response of the supercapacitor cell of each binder. The CV curves of both SBR sample and PTFE sample express rectangular and proportionally balanced shape without any faradaic peaks. As the scan rates increase, the area of rectangular model gradually augments. All of the samples do not have noticeable redox peaks but hardly detectable extensive peaks, which manifest that the signal of charge swap between the electrode and the electrolyte is unconstrained from the given voltage. Moreover, the graphics of CV seem like symmetric shape and it means that the cycling system of supercapacitors is considerably reversible [8,17,19].

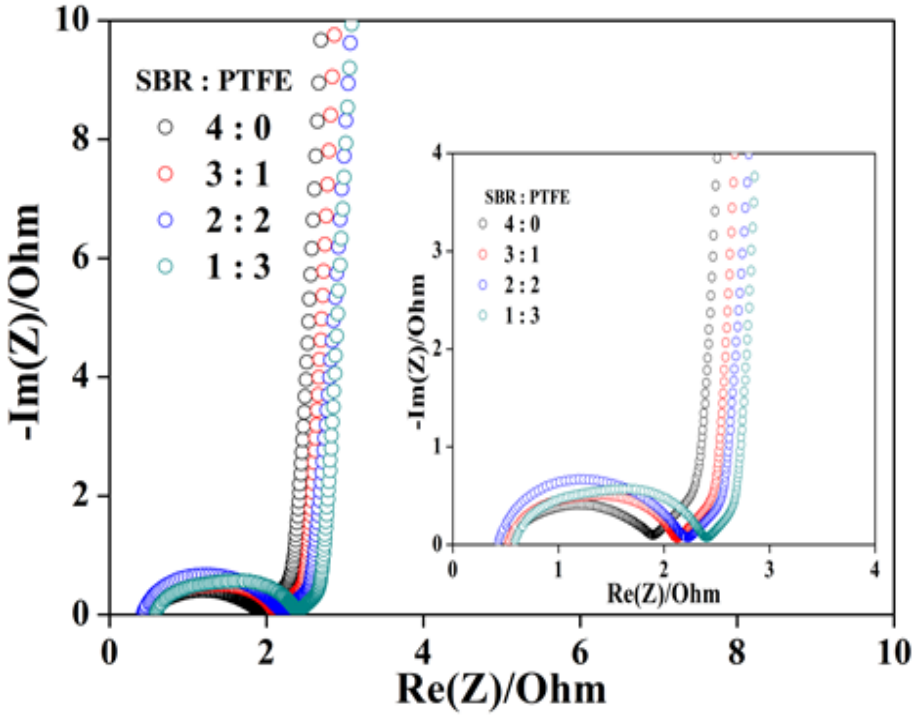

Figure 22. EIS data expressed as Nyquist plot with the frequency range from 10^{-2} to 10^{6} Hz, after 10,000 cycles at 0V.

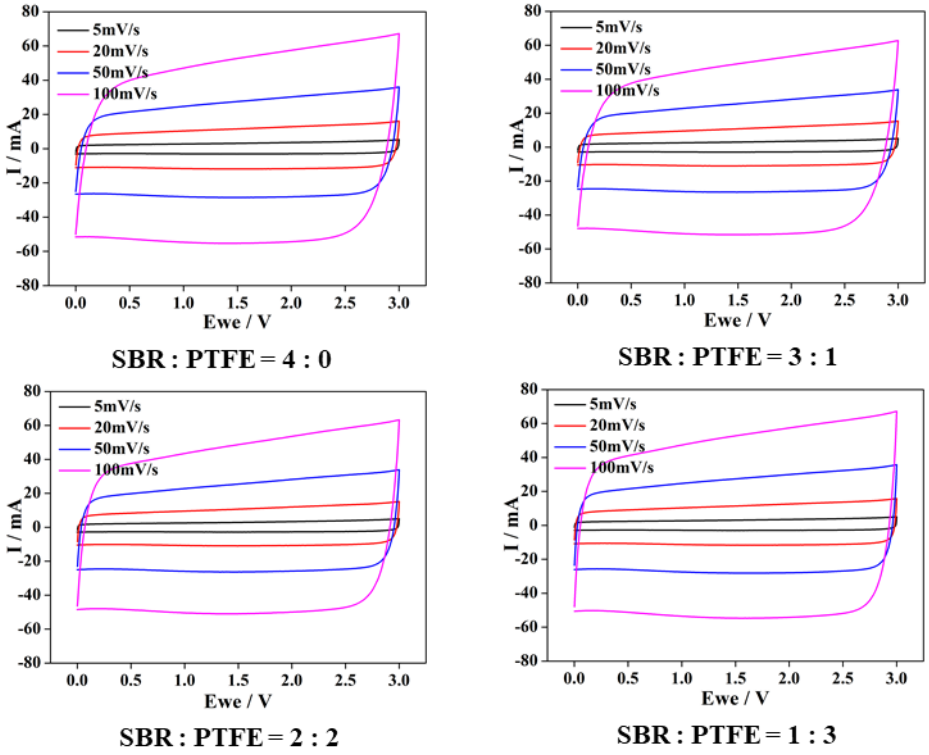

Figure 23. Cyclic voltammograms of the symmetrical supercapacitors with each binders over a voltage in 0-3V, with different scan rates, 5 mV/s, 20 mV/s, 50 mV/s, 100 mV/s.

To see the performance of rate capability at high temperature, Figure 24, all ratios of binder sample were cycled with different current densities at 45℃. In contrast with Figure 21, the electrode having more PTFE amount of binder has high capacitance in rate capability test at 45℃. According to Figure 9, PTFE has good thermal stability, so it does good work at high temperature. SBR:PTFE = 1:3 indicates the highest specific capacitance more than 100F/g at 1mA/cm^2. Also in all range of current density, SBR: PTFE = 1:3 sample has the highest specific capacitance than other samples. The specific capacitances decrease when the electrodes contain more amount of SBR binder. In this regard, SBR: PTFE = 4:0 sample has the lowest cycle performance at the high temperature, but Figure 21 shows that SBR: PTFE = 4:0 sample displays the high specific capacitance over than 100F/g at 1mA/cm^2 at the room temperature. In addition, it has the highest specific capacitance among all samples, even though the given current density is 50mA/cm^2. The specific capacitances of rate capability at high temperature are totally opposite from the test at room temperature. The main factor to cause it is the difference of thermal stability. It can assume that when the temperature increases, it would affect the mechanical structure of active materials. For this reason, the binder which has low thermal stability could disturb ion's movement between active materials and electrochemical double layer by blocking activate porosity [20].

To examine how amounts of resistance are in the electrochemical system at high temperature, EIS test was conducted with the frequency range from 10^{-2} to 10^6 Hz, at 45℃, shown in Figure 25. If the high temperature influences the performance of supercapacitor, the size of semicircle becomes big due to the increment of resistance. A large amount of PTFE would take lower resistance to transfer electrochemical energy between electrode and electrolyte. SBR: PTFE = 1:3 sample has the smallest diameter of a semicircle, but when the electrode includes more SBR, the size of the semicircle is

getting huge. In terms of ESR, the SBR:PTFE = 4:0 sample has 0.524Ω, 3:1 sample has 0.569 Ω, 2:2 has 0.48Ω, and 1:3 sample has 0.476 Ω. The EIS results in Figure 25 are more undesirable than the EIS values in Figure 22. The dissimilarity is an operational environment, so it could be convinced that working temperature concern with the resistance and cycle performance for supercapacitor. The primary cause of performance decline is a variation on the structure of electron storage materials due to the severe operating environments. If the system of the active material was collapsed by exterior factors, the activated surface area of active material would have changed. As a result of this situation, it would be arduous for ions and electrons to transfer their energy toward the target place. The SBR: PTFE = 4:0 sample has relatively enormous resistance, so it means that the collapse degree of the structure much larger than other electrodes which include a great deal of PTFE.

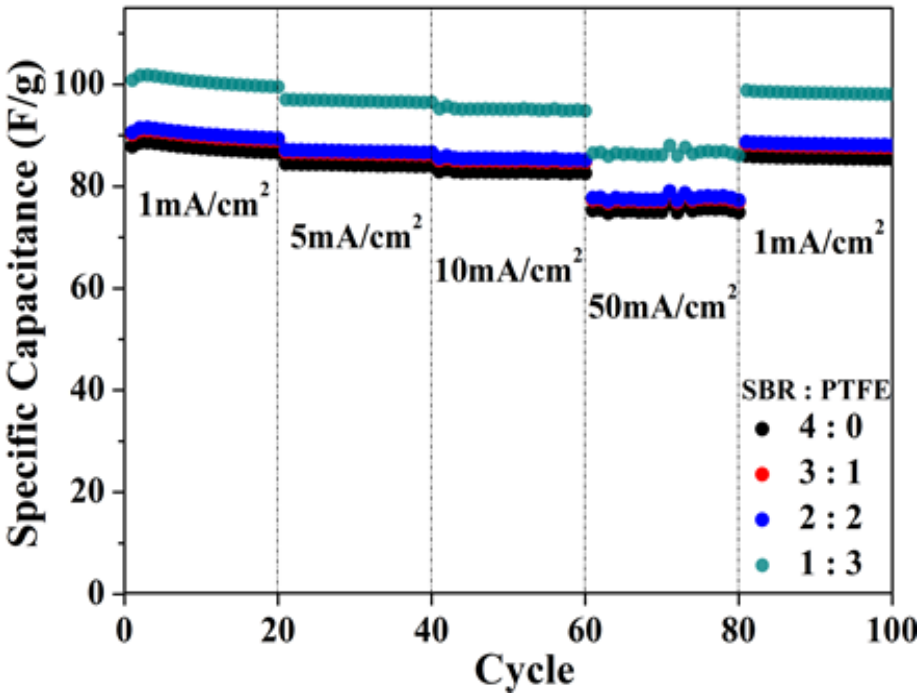

Figure 24. Performance of rate capability with different current density for 20 cycles and voltage range from 0.1 V to 2.7 V at 45 ℃.

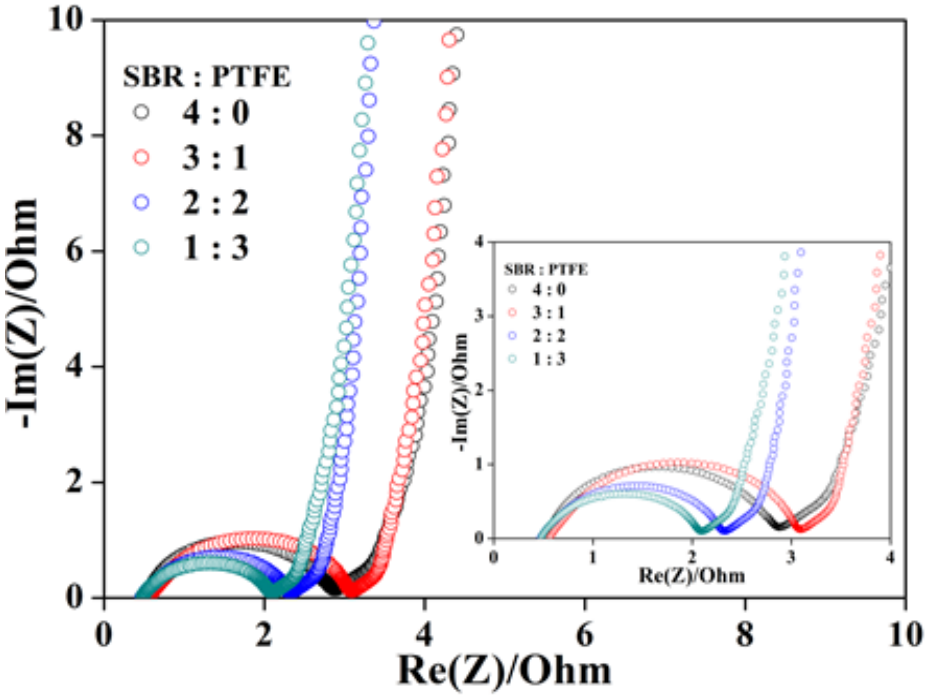

Figure 25. EIS data expressed as Nyquist plot with the frequency range from 10^{-2} to 10^{6} Hz, at 45°C.

3.2.2. The electrodes using CMC sole binder

The cyclic performance of carbon electrodes using CMC binders of different MWs and DSs are illustrated in Figure 26. In this experiment, CMC 250-L has the highest specific capacitance and CMC 90-L has the lowest specific capacitance for 5000 cycles. The cyclic performance was conducted with 10mA/F current from 1.35 V to 2.7 V. From the results, it is clear that there is not any tendency of depending on the MWs of CMC because the mid MW, 250,000, of CMC has larger specific capacitance than CMC 90-L and CMC 700-M. However, it could be seen that when the electrode has high MW at the same with the DS of CMC, it has bigger capacitance than the same DS but less MW of CMC. From Figure 14, the adhesive force may not be attributed to the performance of electrodes containing CMC binders. Even though CMC 700-M has the biggest adhesive force, it shows nonsignificant performance in cycling test. However, CMC 250-L is a kind of low adhesive force and it shows noticeable performance. Also from Figure 17, the affinity between binder and electrolyte may not distinctly effect on the performance of cycling because all of CMC binders have similar the degree of contact angle. Moreover, from Figure 19, ionic conductivity among CMC binders also shows no big different value. It may have a little impact on the performance of EDLCs, but from the results, it cannot exactly conclude that. However, from Table 5, the surface area of micro-pores perfectly corresponds to the specific capacitance of the electrodes, thus the most important factor of EDLCs is an activated surface area in electrodes. Indeed, adding binder into the slurry can block the activated pores of the active material, so the suffusion of binder on the surface of the electrode should be considered to determine the number of binders.

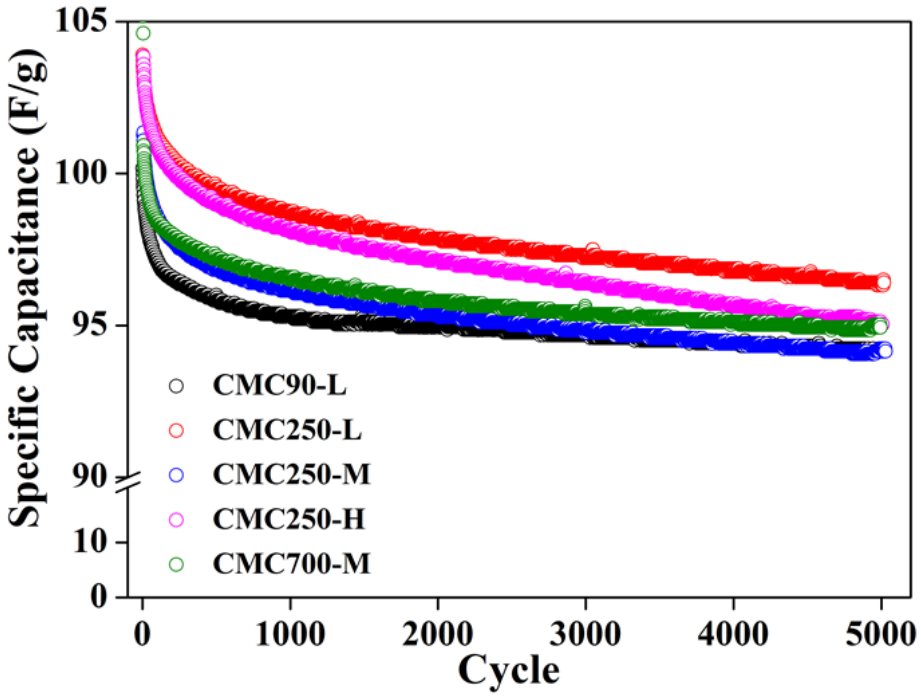

Figure 26. Cyclic performance with a current of 10mA/F from 1.35 V to 2.7 V for 5000 cycles.

In EIS results, we can compare the resistance of depending on MWs and DSs of CMC binders. Figure 27 and the inset explain that the impedance spectra of the EDLCs after 5000 charge/discharge to determine the effect of CMC binder on the resistances of the supercapacitor electrodes. The frequency ranges from 10^{-2} to 10^{6} Hz at 0V. The CMC 250-L has relatively less charge transfer resistance according to the size of semicircle in the middle-frequency region. CMC 250-M has the biggest semicircle in contrast with others, but all Nyquist plots have a similar shape. In terms of ESR, CMC 90-L has 0.493Ω, CMC 250-L has 0.492 Ω, CMC 250-M has 0.466 Ω, CMC 250-H has 0.554 Ω, and CMC 700-M has 0.501 Ω. Even though CMC 250-M indicates the lowest ESR, charge transfer resistance is much enormous than others.

Cyclic voltammetry was conducted by the voltage sweep between 0 and 3 V, with different scan rates. Figure 28 illustrates the cyclic voltammogram response of the supercapacitor electrodes depending on MWs and DSs of CMC binders. The CV curves of all electrodes containing CMC binders draw a rectangular shape without any noticeable peaks. All of the samples do not have faradic redox peaks, moreover, the graphics of CV seem like the symmetric shape and it shows that reversible supercapacitors.

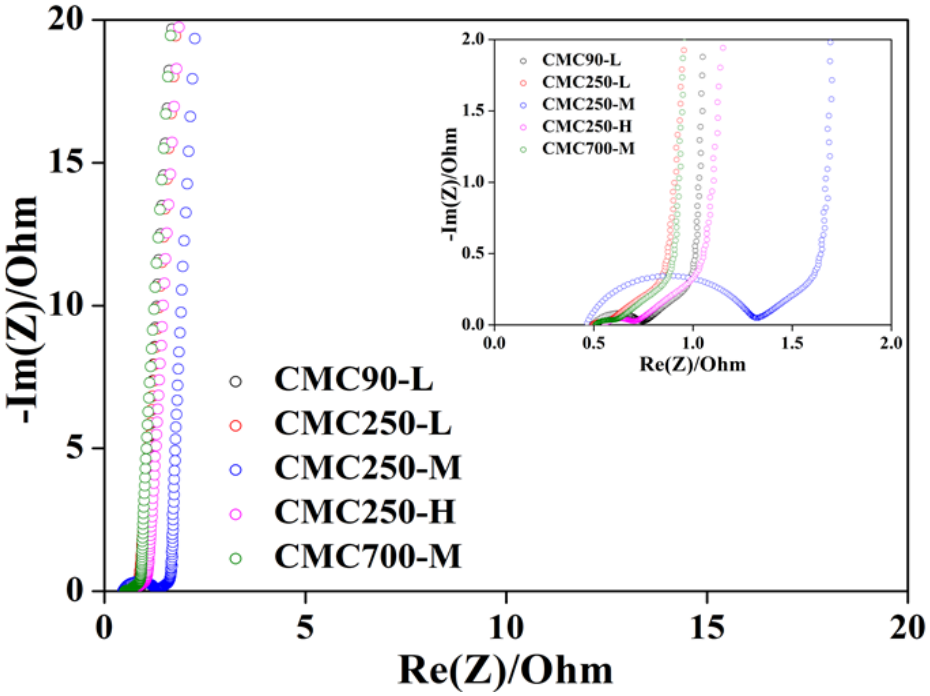

Figure 27. EIS data expressed as Nyquist plot with the frequency range from 10^{-2} to 10^{6} Hz, after 5000 cycles at 0V.

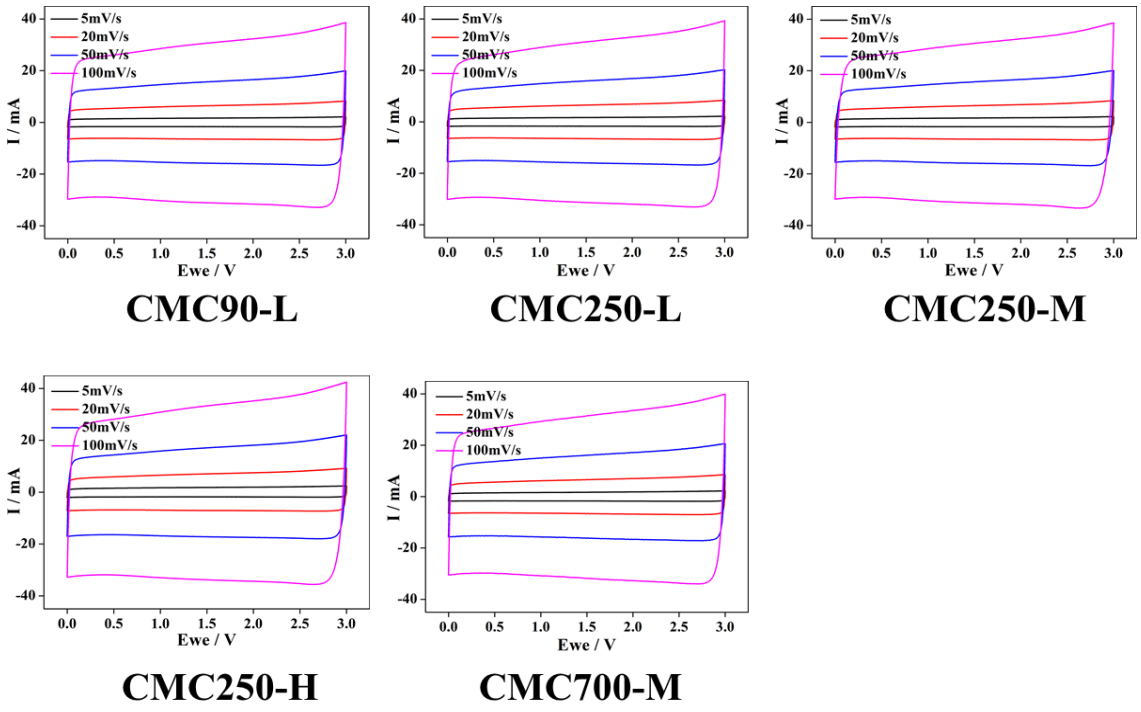

Figure 28. CV data expressed as various scan rate 5mV/s, 20mV/s, 50mV/s, 100mV/s, after the rate capability test.

4. Conclusion

This study investigated several kinds of water-based binder used in EDLCs' electrodes. The effects of binder on the performance of EDLCs system were examined by various electrochemical and physicochemical analysis. The binder covered some portion of active materials, leading to a decrease in BET surface area as well as pore volume. The difference in the coverage according to the ratio of binder materials makes difference in the cyclic performance of EDLC. The surface area of the electrode measured by BET analysis is closely related to the specific capacitance of EDLCs. As expected, less covered electrodes show small internal resistance during cycling and leads to better cyclic performance.

Compared to PTFE, SBR binder makes electrode adhesion stronger and thus holds all components of the electrode relatively for a long time. This eventually gives rise to long life cycle with high power density. In this viewpoint, the SBR binder must be favorable to the EDLCs applied to long-time use. On the contrary, PTFE shows better performance in high temperature so that it is a better choice for the application requiring thermal stability than any other binders. In the case of CMC, its adhesion strength is lower than the combination of SBR and PTFE, but the electrodes containing CMC binder exhibit higher specific capacitance than the electrodes containing SBR and PTFE binders. Consequently, these results are enough to give an initial choice of binder materials for various applications of EDLCs.

5. Reference

[1] X. Sun, X. Zhang, H. Zhang, B. Huang, Y. Ma, Application of a novel binder for activated carbon-based electrical double layer capacitors with nonaqueous electrolytes, J. Solid State Electrochem. 17 (2013) 2035–2042.

[2] A. Burke, Ultracapacitors: why, how, and where is the technology, J. Power Sources. 91 (2000) 37–50.

[3] M. Zhi, C. Xiang, J. Li, M. Li, N. Wu, Nanostructured carbon–metal oxide composite electrodes for supercapacitors: a review, Nanoscale. 5 (2012) 72–88.

[4] L.L. Zhang, X.S. Zhao, Carbon-based materials as supercapacitor electrodes, Chem. Soc. Rev. 38 (2009) 2520–2531.

[5] X. Li, C. Han, X. Chen, C. Shi, Preparation and performance of straw based activated carbon for supercapacitor in non-aqueous electrolytes, Microporous Mesoporous Mater. 131 (2010) 303–309.

[6] I.-J. Kim, S.-Y. Lee, S.-I. Moon, Electric and Mechanical Properties of CMC+PTFE Binary Binder Electrode for Electric Double Layer Capacitor. (2004).

[7] B.-R. Lee, E.-S. Oh, Effect of Molecular Weight and Degree of Substitution of a Sodium-Carboxymethyl Cellulose Binder on Li4Ti5O12 Anodic Performance, J. Phys. Chem. C. 117 (2013) 4404–4409.

[8] C.-M. Wang, C.-Y. Wen, Y.-C. Chen, J.-Y. Chang, C.-W. Ho, K.-S. Kao, W.-C. Shih, C.-M. Chiu, Y.-A. Shen, The Influence of Specific Surface Area on the Capacitance of the Carbon Electrodes Supercapacitor, in: 3rd Int. Conf. Ind. Appl. Eng. 2015 ICIAE2015, 2015.

[9] W.-C. LIAO, F.-S. LIAO, C.-T. TSAI, Y.-P. YANG, Preparation of Activated Carbon for Electric Double Layer Capacitors, China Steel Technical Report, No. 25. pp. 36-41.

(2012).

[10] C. Saka, BET, TG–DTG, FT-IR, SEM, iodine number analysis and preparation of activated carbon from acorn shell by chemical activation with ZnCl2, J. Anal. Appl. Pyrolysis. 95 (2012) 21–24.

[11] A. Balducci, R. Dugas, P.L. Taberna, P. Simon, D. Plée, M. Mastragostino, S. Passerini, High temperature carbon–carbon supercapacitor using ionic liquid as electrolyte, J. Power Sources. 165 (2007) 922–927.

[12] N. Böckenfeld, S.S. Jeong, M. Winter, S. Passerini, A. Balducci, Natural, cheap and environmentally friendly binder for supercapacitors, J. Power Sources. 221 (2013) 14–20.

[13] C. Lämmel, M. Schneider, M. Weiser, A. Michaelis, Investigations of electrochemical double layer capacitor (EDLC) materials – a comparison of test methods, Mater. Werkst. 44 (2013) 641–649.

[14] P. Kurzeil, M. Chwistek, R. Gallay, Electrochemical and Spectroscopic Studies on Rated Capacitance and Aging Mechanisms of Supercapacitors, 2nd European Symposium on Super Capacitors & Applications (ESSCAP), Lausanne, 2 – 3 November. (2006).

[15] C. Portet, P.L. Taberna, P. Simon, C. Laberty-Robert, Modification of Al current collector surface by sol–gel deposit for carbon–carbon supercapacitor applications, Electrochimica Acta. 49 (2004) 905–912.

[16] J. Zhou, W. Xing, S. Zhuo, Y. Zhao, Capacitive performance of ordered mesoporous carbons with tunable porous texture in ionic liquid electrolytes, Solid State Sci. 13 (2011) 2000–2006.

[17] X. Pan, G. Ren, M.N.F. Hoque, S. Bayne, K. Zhu, Z. Fan, Fast Supercapacitors Based on Graphene-Bridged V2O3/VOx Core–Shell Nanostructure Electrodes with a Power Density of 1 MW kg−1, Adv. Mater. Interfaces. 1 (2014) n/a-n/a.

[18] H. Wu, Z. Lou, H. Yang, G. Shen, A flexible spiral-type supercapacitor based on ZnCo2O4 nanorod electrodes, Nanoscale. 7 (2015) 1921–1926.

[19] R. Farma, M. Deraman, Awitdrus, I.A. Talib, R. Omar, J.G. Manjunatha, M.M. Ishak, N.H. Basri, B.N.M. Dolah, Physical and electrochemical properties of supercapacitor electrodes derived from carbon nanotube and biomass carbon, Int. J. Electrochem. Sci. 8 (2013) 257–273.

[20] R. Kötz, M. Hahn, R. Gallay, Temperature behavior and impedance fundamentals of supercapacitors, J. Power Sources. 154 (2006) 550–555.